



Myeloid differential protein-2 inhibition improves diabetic cardiomyopathy via p38MAPK inhibition and AMPK pathway activation

Jianchang Qian^{a,*}, Fei Zhuang^{a,1}, Yujing Chen^{a,1}, Xinrong Fan^a, Jun Wang^b, Zhe Wang^c, Yi Wang^a, Mingjiang Xu^a, Aleksandr V. Samorodov^d, Valentin N. Pavlov^d, Guang Liang^{a,e,**}

^a Chemical Biology Research Center, School of Pharmaceutical Sciences, Wenzhou Medical University, Wenzhou, Zhejiang 325035, China

^b Department of Cardiology, Wenzhou Central Hospital and Affiliated Dingli Clinical Institute, Wenzhou Medical University, Wenzhou 325035, Zhejiang, China

^c Department of Pharmacy, The Second Affiliated Hospital and Yuying Children's Hospital of Wenzhou Medical University, Wenzhou, Zhejiang 325000, China

^d Department of Pharmacology, Bashkir State Medical University, Ufa City, 450005, Russia

^e School of Pharmacy, Hangzhou Medical College, Hangzhou, Zhejiang, China

ARTICLE INFO

Keywords:

Chalcone
Differentiation protein 2
P38MAPK
AMPK
Diabetic cardiomyopathy

ABSTRACT

Myeloid differential protein-2 (MD2) has been shown to play a critical role in the progression of diabetic cardiomyopathy (DCM). This study aims to explore the non-inflammatory mechanisms mediated by MD2 in DCM and to test the therapeutic effects of MD2 inhibitor C30 on DCM. Streptozotocin (STZ) was used to construct DCM model in wild-type and MD2 knockout mice. The collected heart samples were subjected to RNA-sequencing assay. Gene set enrichment analysis of the RNA-seq data indicated that MD2 knockout was associated with energy metabolism pathways in diabetic mouse heart. Further data showed that AMPK pathway was impaired under high glucose condition, which was mediated by p38MAPK activation. MD2 knockout or pharmacological inhibitor C30 completely rescued AMPK signaling through p38MAPK inhibition. Importantly, C30 treatment significantly prevented myocardial damage and dysfunction in T1DM mice evidenced by improved cardiac function and reduced cardiomyocyte apoptosis and cardiac fibrosis. Furthermore, the therapeutic effect of C30 on DCM was correlated to p38MAPK inhibition and AMPK pathway activation *in vivo* and *in vitro*. In conclusion, MD2 inhibition exhibits therapeutic effects on DCM through p38MAPK inhibition and AMPK activation, which enables MD2 a promising target for DCM treatment by suppressing metaflammation and improving cardiac metabolism.

1. Introduction

Diabetic cardiomyopathy (DCM) is a life-threatening specific cardiomyopathy with main clinical outcome of heart failure [1]. A population-based cross-sectional survey demonstrated that the

incidence of DCM is 1.1% (16.9% in diabetic patients), and the cumulative mortality is about 18% [2]. However, there is no specific treatment for DCM except for the application of hypoglycemic drugs and renin-angiotensin system inhibitors [3]. What's worse, the prognosis of DCM is commonly poor even with intensive blood glucose management

Abbreviations: ACC, Acetyl-coenzyme A carboxylase; AGEs, Glycosylation end products; AMPK, AMP-activated protein kinase; ANP, Atrial natriuretic peptide; BAX, BCL2-Associated X; BNP, Type B natriuretic peptide; BSA, Bovine serum albumin; CK-MB, Creatinine kinase MB; CMC-Na, carboxymethyl cellulose sodium; COL-1, collagen I; CPT1A, Carnitine Palmitoyltransferase 1A; DAPI, 4',6-Diamidino-2-Phenylindole, Dihydrochloride; DCM, Diabetic cardiomyopathy; DMEM, Dulbecco's Modified Eagle Medium; DMSO, Dimethyl sulfone; DMSO, dimethyl sulfoxide; FFA, Free fatty acids; GAPDH, glyceraldehyde-3-phosphate dehydrogenase; GO, Gene ontology; GSEA, Gene Set Enrichment Analysis; H&E, Hematoxylin and Eosin; KEGG, Kyoto Encyclopedia of Genes and Genomes; LDH, Lactate dehydrogenase; MAMPs, Metabolic-related molecular patterns; MAPKs, Mitogen-activated protein kinases; MD2, Myeloid differentiation protein 2; mTOR, Mammalian target of rapamycin; MyHC, Myosin heavy chain; NLRP3, NLR family pyrin domain containing protein 3; OxLDLs, Oxidized low-density lipoproteins; SDS-PAGE, Sodium dodecyl sulfate-polyacrylamide gel electrophoresis; SGLT-2, Sodium-glucose cotransporter 2; SREBP1, Sterol regulatory element binding protein-1; STZ, Streptozotocin; T1DM, Type 1 diabetes mellitus; TLRs, Toll-like receptors; α -HBDH, α -hydroxybutyrate dehydrogenase.

* Corresponding author.

** Correspondence to: G. Liang, Chemical Biology Research Center, School of Pharmaceutical Sciences, Wenzhou Medical University, Wenzhou 325035, China.

E-mail addresses: qianjc@wmu.edu.cn (J. Qian), wzmclianguang@163.com (G. Liang).

¹ These authors contributed equally to the work.

<https://doi.org/10.1016/j.bbadis.2022.166369>

Received 24 August 2021; Received in revised form 14 January 2022; Accepted 8 February 2022

Available online 15 February 2022

0925-4439/© 2022 Elsevier B.V. All rights reserved.

[4,5]. Therefore, it is enduring unmet need in DCM treatment, and it is urgent to understand the pathogenesis of DCM to reveal novel therapeutic targets for drug development. In the diabetic status, the overloading of energetic substance dramatically increase the metabolic-related molecular patterns (MAMPs), such as glycosylation end products (AGEs), oxidized low-density lipoproteins (OxLDLs), and free fatty acids (FFA) [6]. These MAMPs cause microvascular damage and eventually the characteristic pathological changes of heart [7,8]. Among which, a chronic low-grade inflammation caused by excess nutrients and metabolites, also known as metaflammation, is a key pathological mechanism [9,10]. MAMPs-induced metaflammation is generally mediated by toll-like receptors (TLRs). Our previous data demonstrated that AGEs can directly bind to myeloid differentiation protein 2 (MD2), an assistant protein of TLR4, and subsequently activated NF- κ B via MyD88-dependent signaling leading to myocardial inflammatory injury [11]. Therefore, MD2/TLR4 inhibition has been considered as a potential therapeutic target for DCM via reducing chronic inflammation in hearts [11,12].

Damaged myocardium energy metabolism is another important pathogeny of DCM [13]. AMP-activated protein kinase (AMPK) is a key functional intracellular protein that regulates the energy homeostasis. Recent evidences have established the relationship between AMPK and DCM [14–16]. The data showed that AMPK activity was significantly inhibited in the myocardium of type 1 diabetic mice, accompanied by cardiac dysfunction. Moreover, genetic inhibition of AMPK can exacerbate myocardial damage and increase mortality in mice with diabetes [17]. These results implied that activating AMPK may be a potential treatment strategy for DCM. Oral administration of the classic hypoglycemic drug metformin showed a potent anti-DCM effect, at least partly via activating AMPK [18,19]. Interestingly, AMPK also interacts with other pathways, such as mitogen-activated protein kinases (MAPKs), NLR family pyrin domain containing protein 3 (NLRP3), etc. [20–22]. These studies demonstrated that in the pathological process of DCM, stress-response pathways can cross talk with other signaling transductions. Therefore, multi-point targeted regulation may be more effective for the treatment of DCM.

Considering the possible interaction between inflammatory signaling and energy metabolism pathway, this study was intent to explore the relationship between MD2 and AMPK in DCM. Furthermore, our group have previously designed and synthesized a series of small-molecule MD2 specific inhibitors, among which, a compound named as C30, (E)-2,3-dimethoxy-4'-methoxychalcone, showed high anti-inflammatory activity in LPS-challenged macrophages through binding the hydrophobic pocket of MD2 [23,24]. Here, the MD2 inhibitor C30 was used to explore the cross-talk of MD2 and AMPK in DCM models. We tested the pharmacological effects of C30 against DCM and investigated the p38-AMPK-involved mechanism.

2. Materials and methods

2.1. Chemicals and reagents

C30 was synthesized and structurally identified in the Chemical Biology Research Center of Wenzhou Medical University as described previously [23]. Recrystallization was performed using CHCl_3 /Ethanol solution to prepare the high purity C30 (>99%) and confirmed by HPLC. SP600125, SB203580, PD98059, AICAR and dorsomorphin were purchased from MedChemExpress (MCE, NJ). Dimethyl sulfoxide (DMSO) was obtained from Sigma-Aldrich (St. Louis, MO). The stock solution (20 mM) was formulated in DMSO and stored at -80°C .

2.2. Transcriptomic sequencing analysis

RNA was extracted from tissues following the standard method. The purity and integrity of RNA were assessed by spectrophotometer and Agilent 2100 bioanalyzer. Then, the library was constructed and

quantified by Qubit 2.0 fluorometer. Next, the effective concentration of library was prepared and subjected to Illumina sequencing. After raw data filtering, sequencing error rate check, and GC content distribution check, clean reads for subsequent analysis are obtained. The featureCounts tool in the subread software was applied to count the number of reads covered by each gene (including the new predicted gene) from the start to the end according to the position information of the gene alignment on the reference genome. To obtain differential expressed genes, the original read count is normalized firstly. Then the statistical model calculates the hypothesis test probability (P value), and finally performs multiple hypothesis test corrections to obtain the FDR value. $|\log_2(\text{FoldChange})| > 1$ & $\text{padj} < 0.05$ were considered as the screening criteria for differential genes. Kyoto Encyclopedia of Genes and Genomes (KEGG), gene ontology (GO) and Gene Set Enrichment Analysis (GSEA) were performed according to the protocol released [25–27].

2.3. Cell culture and treatment

Rat cardiomyocyte-like H9C2 cell line was obtained from the National Collection of Authenticated Cell Cultures (Shanghai, China), and cultured in DMEM (Gibco, ThermoFisher, MA, USA) containing 10% fetal bovine serum, 100 U/mL penicillin, 100 $\mu\text{g}/\text{mL}$ streptomycin at 37°C with 5% CO_2 . H9C2 cell line was adaptively cultured in DMEM (low glucose, 1 g/L) medium. The cells were pretreated with the compounds for 2 h at designed concentration, then stimulated by high concentration of glucose (HG, 40 mM).

2.4. TUNEL assay

H9C2 cells was seeded on glass slides in a 24-well plate. After treatment, the slide was washed with PBS, and fixed in 4% paraformaldehyde for 30 min. Thereafter, incubate the slide with 0.3% TritonX-100 at room temperature for 5 min. Subsequently, dropwise TUNEL solution (Beyotime, Beijing, China) to each slide, and incubate in the dark for 60 min. Finally, the slide was stained with DAPI, and viewed under the fluorescence microscope (excitation wavelength 450–500 nm, emission wavelength 515–565 nm).

2.5. Determination of cell apoptosis

Annexin V-PE Apoptosis Detection Kit was purchased from BD biosciences pharmingen (San Diego, CA). The cells were seeded into 6-well plates at the confluence of 30%. Cells were pretreated with C30 for 30 min, and then stimulated with HG for another 48 h. The cells were harvested and subjected to Annexin V-PE staining following the manufactory instruction. The rate of apoptotic cells were determined by flow cytometry.

2.6. Animal model

C57BL/6 male mice were purchased from Shanghai Slack Laboratory Animal Co., Ltd. (Shanghai, China). MD2 deficiency mice (C57BL/6 background, Strain: B6.129P2-Ly96 <tmlKmy>) were obtained from RIKEN BioResource Research Center (RBRC02388, Japan) and bred in the animal center of Wenzhou Medical University according to the animal care and experimental procedures approved by Wenzhou Medical University animal policy and welfare committee. During the experimental period, the mice were subjected to regular circadian rhythm (light: dark = 12:12 h), and ad libitum to water and food. The temperature of the housing environment is constant at $22 \pm 2.0^\circ\text{C}$, and the humidity is $50\% \pm 5\%$.

For preparation of type 1 diabetes mellitus (T1DM) mouse model, streptozotocin (STZ) formulated in 100 mM citrate buffer (pH 4.5) was intraperitoneally injected for 5 consecutive days at the dose of 50 mg/kg. Before each injection, the mice were fastened overnight (about 12 h). One week after final administration, fasting blood glucose was measured

with the tail vein blood using a glucometer (Omnitest® plus, B. Braun sharing expertise, Hessen, Germany). Blood glucose >12 mmol/L was considered as successful T1DM model. Only mice with at least two consecutive blood glucose tested at >12 mmol/L were used in the study.

For C30 treatment study, mice were divided into 4 groups with at least 6 mice in each group, including control, T1DM, T1DM + C30 at 5 mg/kg and T1DM + C30 at 10 mg/kg groups. C30 or vehicle (0.5% CMC-Na) were given by gavage qod for 16 weeks after establishment of T1DM by STZ injection (blood glucose >12 mmol/L). Two hours after the final dosing, mice were sacrificed. The blood and heart samples were collected and processed for further analyses. For MD2^{-/-} knockout mouse study, mice were grouped into MD2^{-/-}, MD2^{-/-} + T1DM, Control, and T1DM groups. After T1DM established for 2 weeks, the mice were fed for another 16 weeks and then sampled, totally as previously reported by our group [11].

2.7. Serological testing for cardiac function

Sera were isolated by centrifuge at 3000 × rpm, 4 °C for 15 min, and subjected to creatinine kinase MB (CK-MB), α-hydroxybutyrate dehydrogenase (α-HBDH) and lactate dehydrogenase (LDH) detection following the manufactory instructions (Nanjing Jiancheng Bioengineering Institute, Nanjing, China).

2.8. Echocardiography

Three days before mice were sacrificed, cardiac function was evaluated by transthoracic echocardiography. The acuson-sequoia 512 was equipped with an acuson 15L8W ultrasound transducer linear probe setting at the frequency ranged in 12–14 MHz. Representative M-mode and short-axis views were captured. To determine the diastolic function, pulsed-wave doppler imaging of the transmitral filling pattern was performed.

2.9. Histological examination

The apex of heart was fixed in 4% paraformaldehyde. Tissues were dehydrated using gradient ethanol ranging from 70% to 100%. Subsequently, embedded in paraffin and cut into 5 μm thickness sections. The paraffin sections were prepared and subjected to hematoxylin and eosin (H&E) staining. Masson's trichrome staining kits was purchased from Solarbio Science & Technology Co., Ltd. (Beijing, China). The stained sections were observed using an optical microscope (Nikon, Tokyo, Japan), and the image was captured. The fibrotic area was measured using a quantitative digital image analysis system (Image-Pro, NIH, Bethesda, MD).

For immunofluorescence staining, the paraffin section was sequentially deparaffinized and hydrated. After antigen retrieval in saturated sodium citrate buffer (10 mM, pH 6.0) for 3 min using high pressure steam method, sections were further incubated in 3% H₂O₂ for 30 min. Subsequently, block the slides with 5% BSA buffer for 30 min. The primary antibody was diluted using 5% BSA buffer, and then incubated in working solution of primary antibody at 4 °C for overnight. Thereafter, the section was washed and further incubated with fluorescent labeled secondary antibody (ThermoFisher, MA, USA) for 1 h at room temperature. Wash the section with PBS and mount with anti-fluorescence quencher buffer that containing DAPI (Beyotime biotechnology, Shanghai, China). The image was viewed and captured by fluorescence microscope (Nikon, Tokyo, Japan). The representative images were quantified by Image-Pro [28].

2.10. Real-time quantitative PCR

Total RNA of each sample was extracted following the manufacturer's protocol with TRIzol (Invitrogen, CA, USA) and cDNA were synthesized with M-MLV reverse transcriptase (Invitrogen, CA, USA).

Quantitative PCR was performed using platinum® SYBR® Green qPCR SuperMix-UDG (Invitrogen, CA, USA) on Eppendorf Mastercycler®ep realplex detection system (Hamburg, Germany). Primers for the target gene (Supplementary Table S1) were synthesized by Invitrogen (Shanghai, China). The transcriptional level of each gene was normalized to β-actin.

2.11. Western blot

The lysate extracted from cells or heart tissues was separated by 10% SDS-PAGE, and electrotransferred onto the nitrocellulose membrane (Millipore, MA, USA). Then, the NC membrane was blocked with 5% skimmed milk at ambient temperature for 2 h, and then incubated with primary antibodies and secondary antibodies successively. Finally, the blot was visualized using enhanced chemiluminescence reagents (Bio-Rad, CA). The specific band was further quantified by Image J software and normalized to the loading control. Primary antibodies, including p-AMPK (Thr172), AMPK, p-p38MAPK, p38MAPK, p-mTOR, mTOR, p-ACC and GAPDH, were purchased from Cell Signaling Technology (MA). Collagen-I (COL-1), Bax and Bcl-2 antibodies were purchased from Abcam Technology (Massachusetts, MA). Atrial natriuretic peptide (ANP), myosin heavy chain (MyHC), TLR4 and MD2 antibodies were purchased from Santa Cruz Technology (CA). The secondary antibody was obtained from Shanghai Yeasen Biotechnology Company (Shanghai, China).

2.12. Statistic analysis

SPSS 22.0 and Graphpad Prism 8 software were used for statistical analysis and graphing. All data were presented as mean ± SEM. One-way ANOVA followed by Dunnett's post hoc test was carried out for multiple group comparisons. If data follow a non-parametric distribution, a non-parametric Kruskal–Wallis test followed by Dunn's post hoc test was performed. Results were considered as significant at $P < 0.05$.

3. Results

3.1. Transcriptome sequencing highlighted the metabolic pathways modulated by MD2 in DCM

MD2 has been demonstrated to mediate inflammatory damage in diabetic myocardium in our previous study, where MD2 gene knockout significantly attenuated hyperglycemia-induced cardiac dysfunction and cardiomyopathy [11]. To further explore the role of MD2 in DCM, the transcriptome sequencing method was employed to display the differential gene expression using the mouse heart tissues which obtained from our previous work [11]. As shown in Fig. 1A, the expression profile of the T1DM group was distinguished from that of the healthy control group (Control), and the gene expression profile of the MD2^{-/-} T1DM group was close to that of the MD2^{-/-} and Control groups. Compared MD2^{-/-} group with Control group, 2287 genes were significantly up-regulated and 2335 genes were remarkably down-regulated. In addition, 869 genes were up-regulated and 863 genes were down-regulated when comparing T1DM to MD^{-/-}T1DM group (Fig. 1B). Gene set enrichment analysis (GSEA) demonstrated that glucose and lipid metabolism related genes were enriched in the MD^{-/-}T1DM group (Nominal p -value <0.01) (Fig. 1C). These results suggest that MD2 may be cross-linked with energy metabolism pathways in the heart.

3.2. Suppression of MD2 activated AMPK signaling in vitro and in vivo

To confirm the role of MD2 in metabolic signaling pathways revealed by the RNA-seq data, functional proteins that involved in glucose and lipid metabolism, especially AMPK and its downstream proteins mTOR, ACC, and SREBP1, were analyzed in H9C2 cells with or without MD2 knockdown under HG condition. As shown in Fig. 2A, p-AMPK and p-

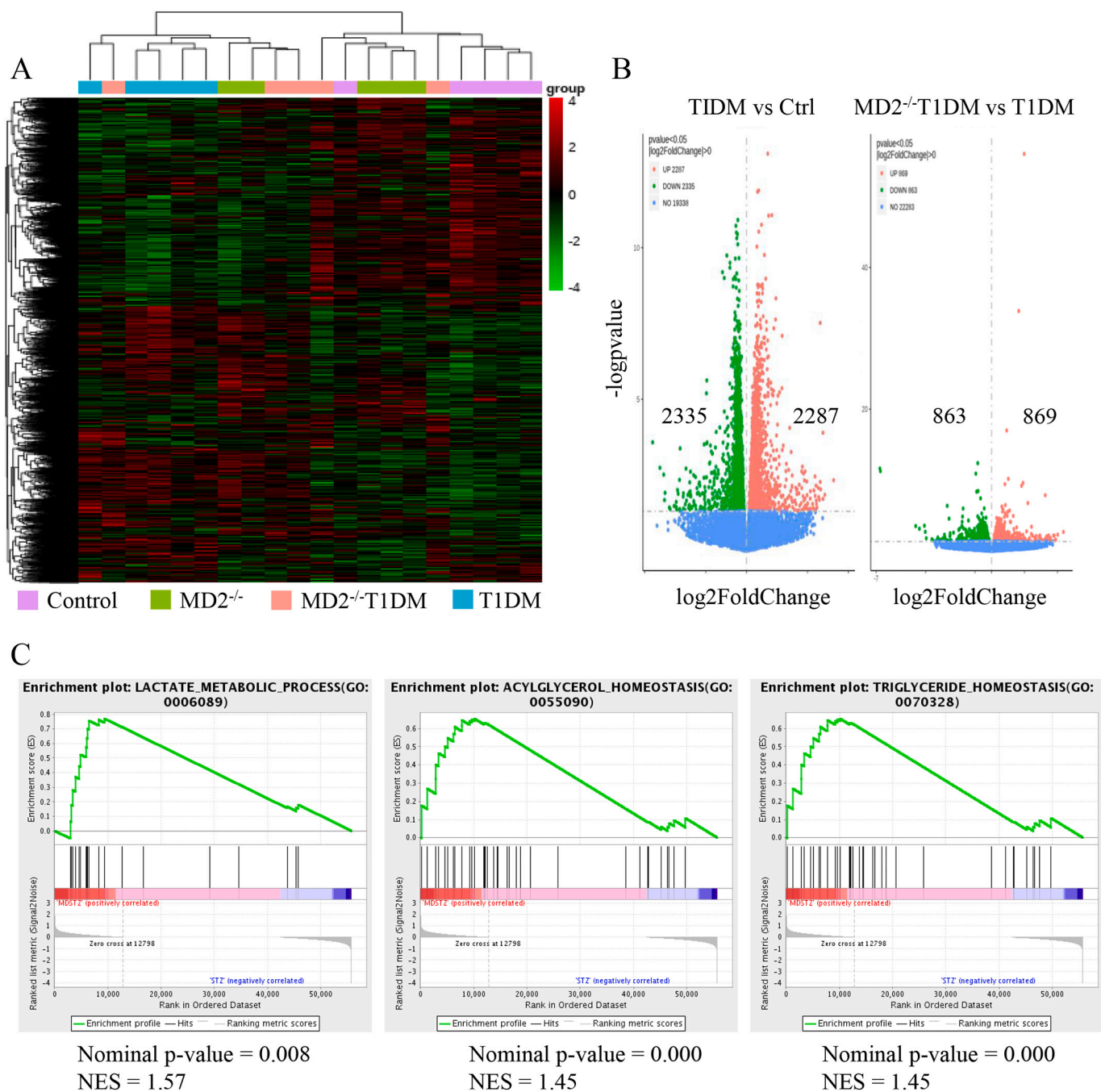


Fig. 1. Transcriptomic sequencing highlighted the metabolic pathway associated with MD2 in DCM. (A) Cluster heatmaps showed the heart RNA-seq results of the mouse hearts from control group, MD2^{-/-} group, MD2^{-/-}T1DM group, and T1DM group in our previous study [11]. (B) Volcano maps showed the differential gene expression of T1DM group versus control group and MD2^{-/-}T1DM groups versus T1DM group, respectively. (C) Gene set enrichment analysis of lactate metabolic process, acylglycerol homeostasis and triglyceride homeostasis. NES means normalized enrichment score.

ACC was remarkably decreased with HG treatment in a time-course manner from 24 to 72 h. The levels of p-mTOR and p-SREBP1c were significantly increased correspondingly (Fig. 2A and Supplementary Fig. S1). Interestingly, when MD2 was knocked down by siRNA (Supplementary Fig. S2), HG-suppressed p-AMPK was completely recovered (Fig. 2B). Like the in vitro results, the level of p-AMPK was significantly reduced ($p < 0.001$) in the myocardial tissue of T1DM mice, which was completely rescued by MD2-deficiency (Fig. 2C and D). These results suggest that MD2 inhibition rescue AMPK activity under HG condition in vitro and in vivo.

3.3. p38MAPK was an upstream regulator of AMPK in DCM

Pathway enrichment analysis on the transcriptome data was conducted to reveal potential signaling pathways that were associated with MD2 deficiency. Firstly, 434 intersectional genes were identified between the up-regulated genes of STZ vs Control and the down-regulated genes of MDST2 vs STZ (Supplementary Fig. S3), and then pathway enrichment analysis was conducted on the 434 genes with the online tool DAVID (Supplementary Tables S2 and S3). These genes were found enrich in dilated cardiomyopathy and hypertrophic cardiomyopathy. MAPK pathway that is closely related to inflammation was also identified in the top enrichment pathways (Fig. 3A). Interestingly, we treated

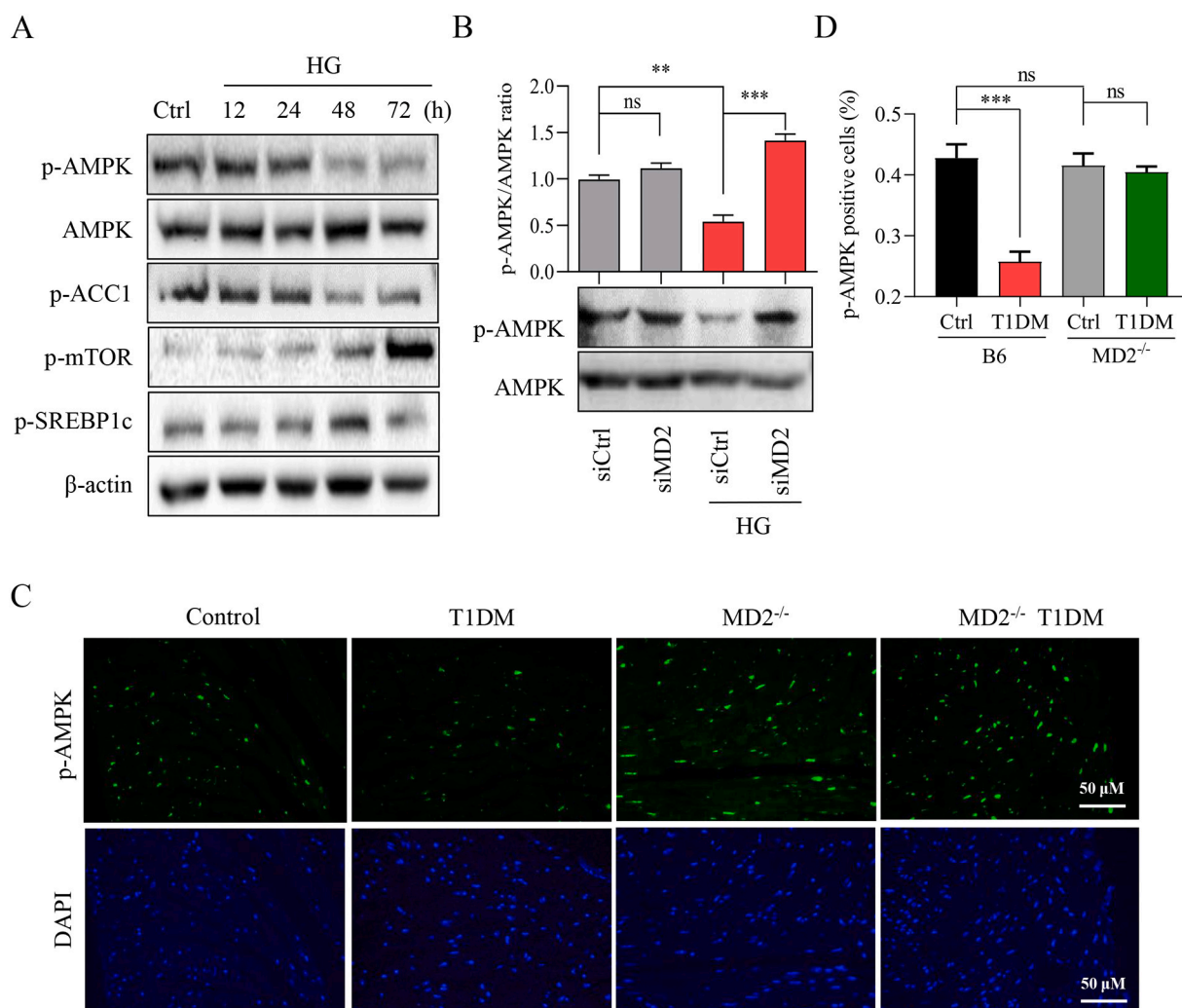


Fig. 2. Blocking MD2 rescued high glucose-repressed p-AMPK in vitro and in vivo. (A) H9C2 cells were cultured in DMEM low-glucose medium, and then stimulated with 40 mM glucose (HG) for the indicated time. p-AMPK, p-ACC1, p-mTOR, p-SREBP1c were detected by western blot. AMPK and β -actin were loading controls. (B) H9C2 cells were transfected with control (siCtrl) or MD2 siRNA (siMD2) for 48 h, and then treated with HG for another 48 h. p-AMPK and AMPK were detected by western blot assay. (C) Representative images of immunofluorescence staining and (D) corresponding percentage of p-AMPK positive cells in the heart tissues of each group were shown. ** $P < 0.01$, *** $P < 0.001$; ns means no significant difference.

H9C2 cells with JNK inhibitor SP600125 (SP), p38MAPK inhibitor SB203580 (SB), and MEK inhibitor PD98059 (PD), respectively, and HG-suppressed p-AMPK was completely blocked with SB treatment (Fig. 3B, Supplementary Fig. S4A). Indeed, the level of p-p38 was dramatically increased 24 h after HG treatment, which was preceded to the decrease of p-AMPK (48-h point) (Fig. 3C). The control group incubated with low glucose for 72 h did not show p38 activation. Furthermore, the increased level of p-p38 was also normalized to the control mice in the MD2 deficient hearts in vivo (Fig. 3D and E). These effects were accompanied with alleviation of hyperglycemia-induced apoptotic pathway activation in the heart. As shown in Fig. 3F, apoptosis-related biomarkers, including cleaved PARP and Bax, were significantly up-regulated in the hearts of diabetic mice, but they were obviously suppressed in MD2^{-/-} mice (Supplementary Fig. S4B).

3.4. C30 promoted myocardial cell survival via p38MAPK/AMPK axis

C30 is a verified MD2 specific small molecule inhibitor [24]. H9c2 cells were pre-treated with C30 and SB and then treated with HG for 24 or 48 h, respectively, according to the time-course results. As shown in Fig. 4A, HG significantly increased p-P38 that was clearly inhibited with C30 (10 μ M) or SB (10 μ M) pre-treatment, and HG-decreased p-AMPK

was rescued by C30 or SB pre-treatment correspondingly (Supplementary Fig. S5A). Moreover, the potency of AICAR to activate AMPK, evidenced by increased p-AMPK and decreased p-mTOR, was comparable to that of C30 under HG condition (Fig. 4B, Supplementary Fig. S5B). However, C30 did not rescue p-AMPK level that was reduced by dorsomorphin, a classic AMPK inhibitor (Fig. 4C, Supplementary Fig. S5C). Next, we examined the effect of C30 on hyperglycemia-induced apoptosis. As shown in Fig. 4D, hyperglycemia induced about 25% of H9C2 cells to undergo apoptosis, and C30 treatment significantly inhibited apoptosis in HG treated H9C2 cells that was comparable to the potency AICAR (Supplementary Fig. S5D and S6). The protective role of C30 and AICAR in HG-induced cell apoptosis was further confirm by TUNEL staining (Fig. 4E).

3.5. C30 suppressed hyperglycemia-induced myocardial apoptosis via activating AMPK

MD2 gene knockout has been reported to attenuate cardiac dysfunction in diabetic mice [11]. To investigate the cardioprotective effects of MD2 inhibitor C30 on DCM in vivo, echocardiography was used to evaluate cardiac function. As shown in Table 1 and Supplementary Fig. S7A–B, C30 treatment significantly improved EF in the

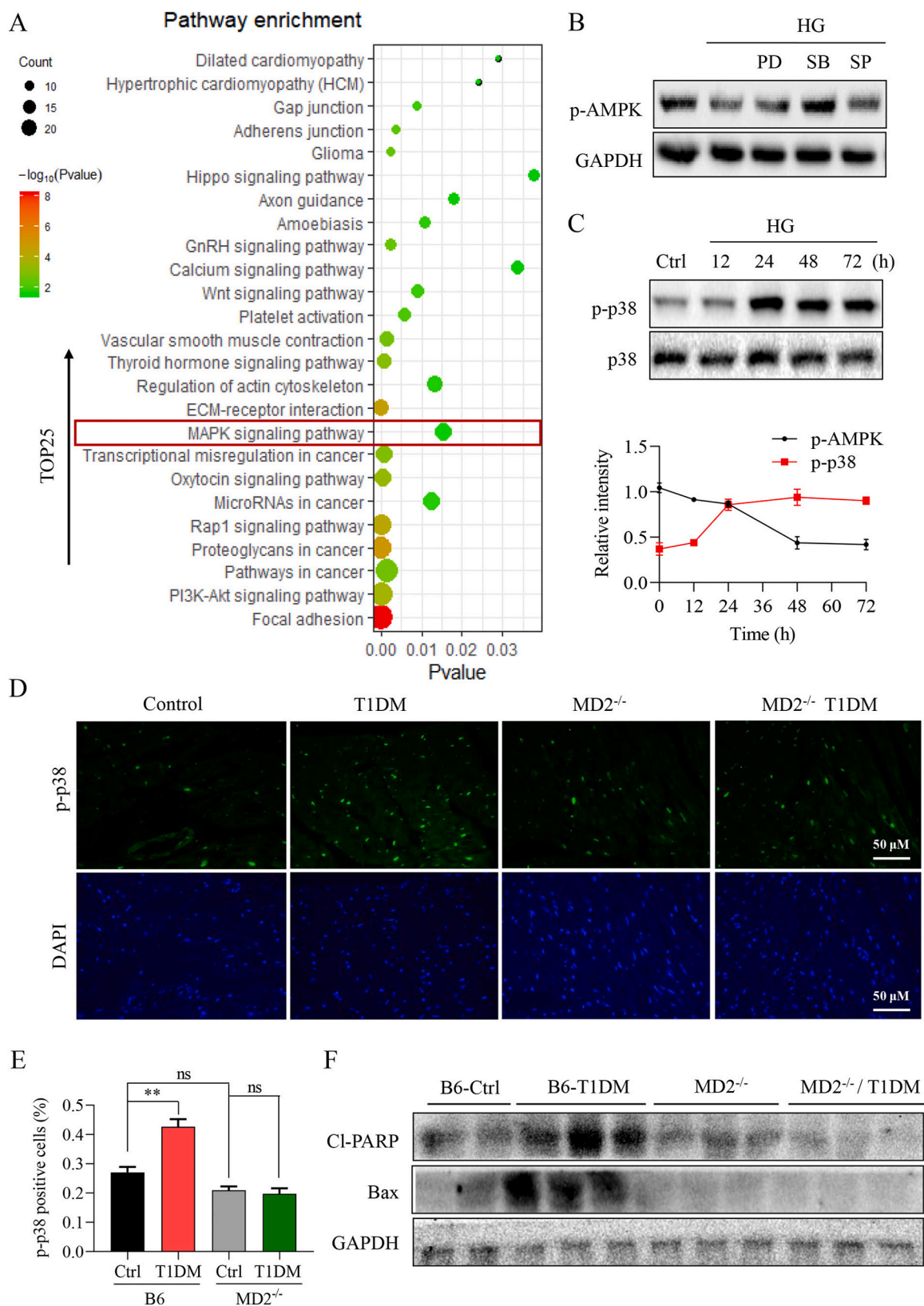


Fig. 3. AMPK activation was a downstream signaling of p-P38 in DCM. (A) Bubble chart of top 25 enriched pathways from KEGG pathway enrichment analysis of the RNA-seq results. (B) H9C2 cells were pretreated with 10 μM PD98059, SB203580 and SP600125, respectively, for 1 h, and then stimulated with HG for another 48 h. p-AMPK, AMPK and GAPDH were detected. (C) H9C2 cells were treated with HG for the indicated time. p-P38 and P38 were determined and quantified. (D-E) Representative images of immunofluorescence staining and (D) corresponding percentage of p-p38 positive cells in the heart tissues of each group were shown. (F) Cleaved-PARP and Bax were detected in the heart tissues. GAPDH was a loading control. ***P* < 0.01; ns means no significant difference.

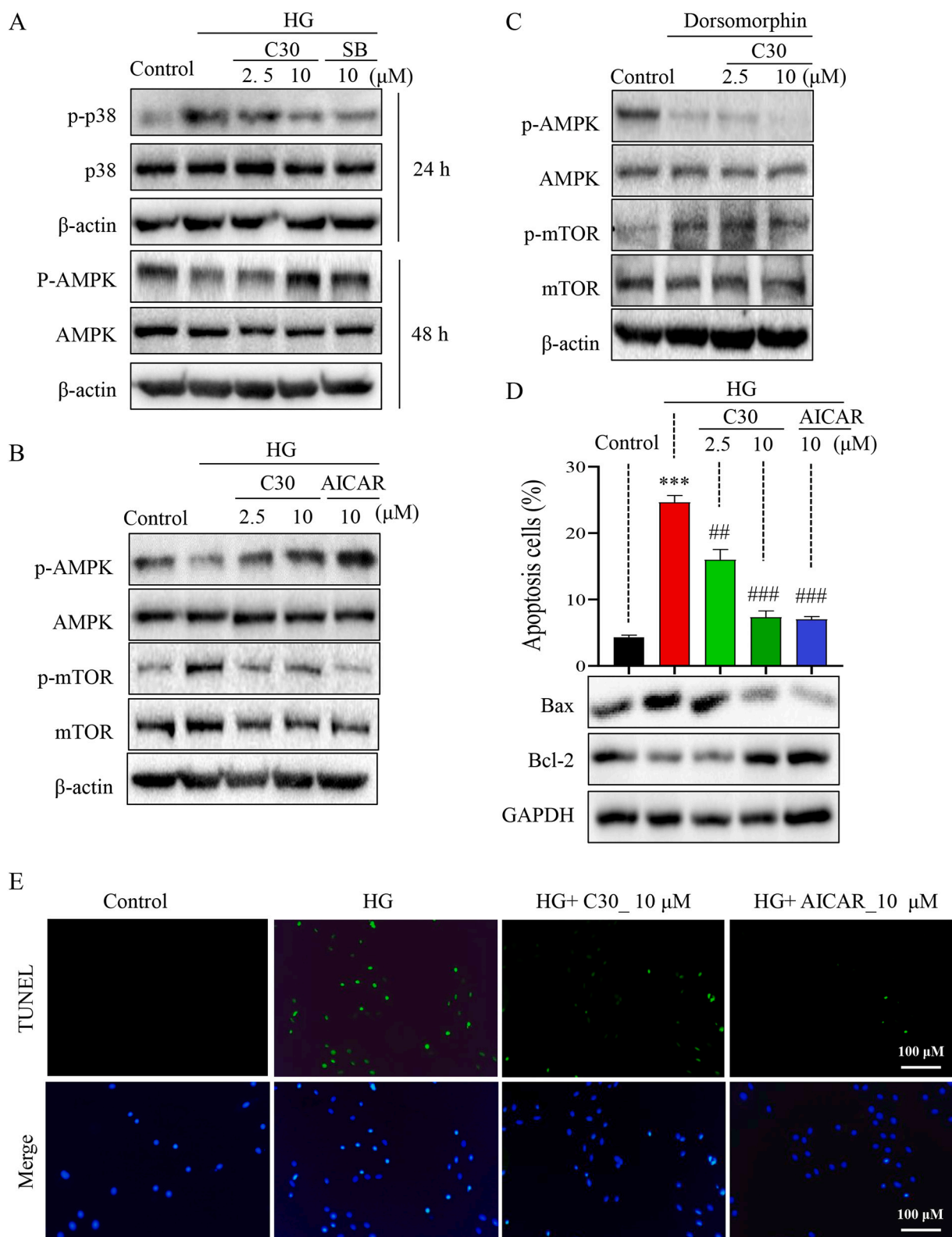


Fig. 4. C30 protected H9C2 from HG induced apoptosis via modulating p38MAPK-AMPK axis. (A-B) H9C2 cells were pretreated with or without C30, SB and AICAR for 1 h, then stimulated with HG (40 mM) for indicated time. p-P38, P-AMPK, p-mTOR were detected by western blot. (C) H9C2 cells were pretreated with C30, and then incubated with 10 μM Dorsomorphin for another 2 h. p-AMPK, AMPK, p-mTOR and mTOR were detected by western blot. (D) H9C2 cells were treated as interpreted in "A", and then the percentage of apoptotic cells were determined by flow cytometry after Annexin V-PE staining (top panel), and Bax and Bcl-2 were detected by western blot (lower panel); GAPDH was a loading control. (E) After 48 h incubation with HG, TUNEL assay was performed. The representative images were shown (400×). ****P* < 0.001 vs control; ##*P* < 0.01, ###*P* < 0.001 vs HG.

Table 1
Echocardiographic parameters of T1DM mice with or without C30 treatment.

| Parameter | Control | T1DM | T1DM + C30 5 mg/kg | T1DM + C30 10 mg/kg |
|-----------|---------------|------------------|--------------------------|--------------------------|
| HR (bpm) | 501.7 ± 13.28 | 400.1 ± 32.03* | 405.0 ± 29.01 | 416.6 ± 9.98 |
| FS% | 44.58 ± 1.5 | 35.40 ± 1.8* | 40.65 ± 2.4 | 41.52 ± 1.4 [#] |
| EF% | 82.37 ± 1.7 | 70.90 ± 2.0* | 77.73 ± 2.7 [#] | 79.13 ± 1.5 [#] |
| E (m/s) | 0.56 ± 0.03 | 0.44 ± 0.06* | 0.38 ± 0.02 | 0.45 ± 0.05 |
| IVSd (mm) | 0.84 ± 0.03 | 0.70 ± 0.01* | 0.76 ± 0.02 | 0.83 ± 0.02 [#] |
| IVSs (mm) | 1.10 ± 0.08 | 0.92 ± 0.02* | 0.94 ± 0.01 | 0.99 ± 0.03 |
| LVd (mm) | 2.6 ± 0.01 | 2.4 ± 0.01* | 2.5 ± 0.01 | 2.6 ± 0.008 [#] |
| LVs (mm) | 1.42 ± 0.003 | 1.58 ± 0.001 | 1.51 ± 0.01 [#] | 1.5 ± 0.009 [#] |
| FWd (mm) | 0.875 ± 0.037 | 0.730 ± 0.009*** | 0.77 ± 0.01 [#] | 0.80 ± 0.02 [#] |
| FWs (mm) | 1.12 ± 0.07 | 0.94 ± 0.02* | 0.97 ± 0.02 | 1.01 ± 0.03 |
| PWd (mm) | 0.84 ± 0.03 | 0.74 ± 0.02* | 0.78 ± 0.02 | 0.80 ± 0.02 |
| PWs (mm) | 1.06 ± 0.04 | 0.95 ± 0.02* | 0.81 ± 0.14 | 1.02 ± 0.04 |

HR, Heart Rate; FS%, Fraction shortening; EF%, ejection fraction; E, peak mitral E velocity; IVSd, interventricular septal dimension in diastole; IVSs, interventricular septal dimension in systole; LVd, left ventricle in diastole; LVs, left ventricle in systole; FWd, left ventricular free wall in diastole; FWs, left ventricular free wall in systole; PWd, posterior wall thickness in diastole; PWs, posterior wall dimension in systole. Data were presented as mean ± SEM, and analyzed by one-way ANOVA. Control vs T1DM, * $P < 0.05$, *** $P < 0.001$. T1DM vs T1DM + C30, # $P < 0.05$, ## $P < 0.01$, $n = 5$.

T1DM mice without influencing on body weight and blood glucose. Further myocardial enzyme assays including CK-MB, α -HBDH and LDH showed that all of the three myocardial enzymes were significantly increased in the sera of the T1DM mice, and C30 treatment significantly reduced the levels of CK-MB, α -HBDH and LDH (Fig. 5A-C). Further qPCR indicated that gene expression levels of MyHC, type B natriuretic peptide (BNP) and COL-1 were significantly increased in the hearts of T1DM mice that were prevented by C30 treatment (Fig. 5D-F). The changes in MyHC and ANP were confirmed at protein levels (Supplementary Fig. S7C). Masson's trichrome staining further revealed clear cardiac fibrosis in the T1DM mice that was ameliorated by C30 treatment (Fig. 5G).

As expected, C30 treatment significantly rescued hyperglycemia-decreased p-AMPK level in the hearts of T1DM mice as shown in the immune staining and western blot (Fig. 6A-B). Similar to the results of the MD2 deficient mice, C30 treatment also clearly ameliorated hyperglycemia-induced P38 phosphorylation, Cl-PARP, and Bax expression in the hearts, but increased BCL-2 level compared to the vehicle treated mice (Fig. 6B). These data indicate that C30 treatment significantly alleviated hyperglycemia caused myocardial damage.

4. Discussion

DCM is mainly characterized by ventricular diastolic dysfunction, cardiomyocytes apoptosis, cardiac fibrosis and remodeling, and finally progresses to heart failure [29]. Previously, we had demonstrated a key role of MD2 in DCM progress through directly binding to AGEs and FFA to activate TLR4/MAPKs/NF κ B pathway, which is an inflammatory mechanism mediated by MD2 in DCM [11,12]. In this study, further in vitro and in vivo data showed that MD2 inhibition rescued AMPK activity under HG condition, which was mediated by p38MAPK activation, which represents a non-inflammatory mechanism mediated by MD2 in DCM. We think that both pathways (inflammatory and non-

inflammatory) mediated by MD2 contribute to the pathogenesis and development of DCM. In addition, MD2 inhibitor C30 treatment significantly prevented myocardial damage and dysfunction in T1DM mice, and we demonstrated a therapeutic effect of C30 on DCM through p38MAPK inhibition and AMPK pathway activation in vivo and in vitro, providing a potential drug candidate for DCM treatment.

Metaflammation caused by MAMPs plays important role in the progress of DCM [6,30]. Although there is no anti-inflammatory drug approved for DCM treatment currently, inhibition of metaflammation is a promising treatment strategy for DCM. Phosphodiesterase 5 inhibitor (Sildenafil) has shown efficacy on improving myocardial remodeling in diabetic patients that is correlated to IL-8 inhibition (ClinicalTrials.gov, NCT00692237). IL-1 β inhibition by monoclonal antibody Canakinumab significantly reduces the incidence of heart failure in patients with diabetes (ClinicalTrials.gov, NCT01327846). Of note, TLR4/NF κ B pathway takes an important role in mediating the inflammatory response of MAMPs [6], and MD2 is a key protein that initiates TLR4-NF κ B signal transduction. The protein level of MD2 has been found to be up-regulated dramatically in the heart of diabetic mouse, indicating a significant relationship between MD2 and DCM [11]. In addition, we have demonstrated that AGEs and palmitic acid can directly bind to MD2 to promote the activation of TLR4 and the downstream signaling MAPKs and NF κ B [11,12]. Both AGEs and FFA are important risk factors of DCM. Therefore, MD2 can be a promising drug target for DCM treatment.

Several MD2 inhibitors have been reported and significantly inhibit LPS-induced inflammatory response, such as JSH, Xanthohumol, caffeic acid phenethyl ester and curcumin [31–34]. These compounds have common structural features and contain chalcone skeleton structure. Therefore, our team synthesized a series of chalcone analog, and C30 is one of the lead compound with high specificity and potent affinity to MD2 [24]. Here we first time to test the efficacy of C30 on DCM. The results showed that C30 treatment significantly prevented hyperglycemia-induced myocardial dysfunction, cardiac fibrosis, and cardiomyocyte apoptosis. Thus, C30 is a potential drug candidate for DCM treatment that however need further development to improve the pharmacokinetic profile. The bioavailability of C30 is 2.89% as low as that of curcumin (Supplementary Fig. S8A–C). The oral half-life of C30 was significantly improved comparing with curcumin, reaching 11 h. Unfortunately, this study did not establish the correlation between C30 blood exposure and drug efficacy (PD-PK study), and further research is still needed.

In addition to chronic inflammation, energy metabolism disorders play a critical role in the progression of DCM. Increased fatty acid intake, triacylglycerol accumulation, and decreased glucose utilization in the heart were observed and correlated to the occurrence and development of DCM [35]. Mechanistically, a number of studies have shown that AMPK activity is significantly reduced and contributes to myocardial hypertrophy and cardiac dysfunction in animals with type 1 or type 2 diabetes [36,37]. Cardiomyocyte-specific AMPK knockout exacerbated cardiac function [38]. AMPK is a key energy sensor and regulates sugar and lipid metabolism in the cells by modulating mTOR signaling pathway, acetyl-coenzyme A carboxylase (ACC), malonyl-CoA, CPT1A, etc. [39–41]. Due to its crucial role in DCM, activation of AMPK is expected to be a therapeutic strategy for DCM intervention. Metformin, a classic oral hypoglycemic agent and a recognized AMPK agonist, can reduce the risk of heart failure and the mortality of diabetic patients [42]. In addition, the beneficial effect of novel hypoglycemic drug sodium-glucose cotransporter 2 (SGLT-2) inhibitors on DCM is proven to be AMPK dependent but not inhibition of SGLT-2 [43]. In this study, impaired AMPK signaling was observed in the hearts of T1DM mice. Interestingly, MD2 knockout or pharmacological inhibitor C30 treatment completely rescued hyperglycemia-impaired AMPK activity in T1DM mice and normalized sugar and lipid metabolism related gene expression. These data indicate that MD2 inhibition alleviates DCM through not only suppressing inflammatory response but also improving

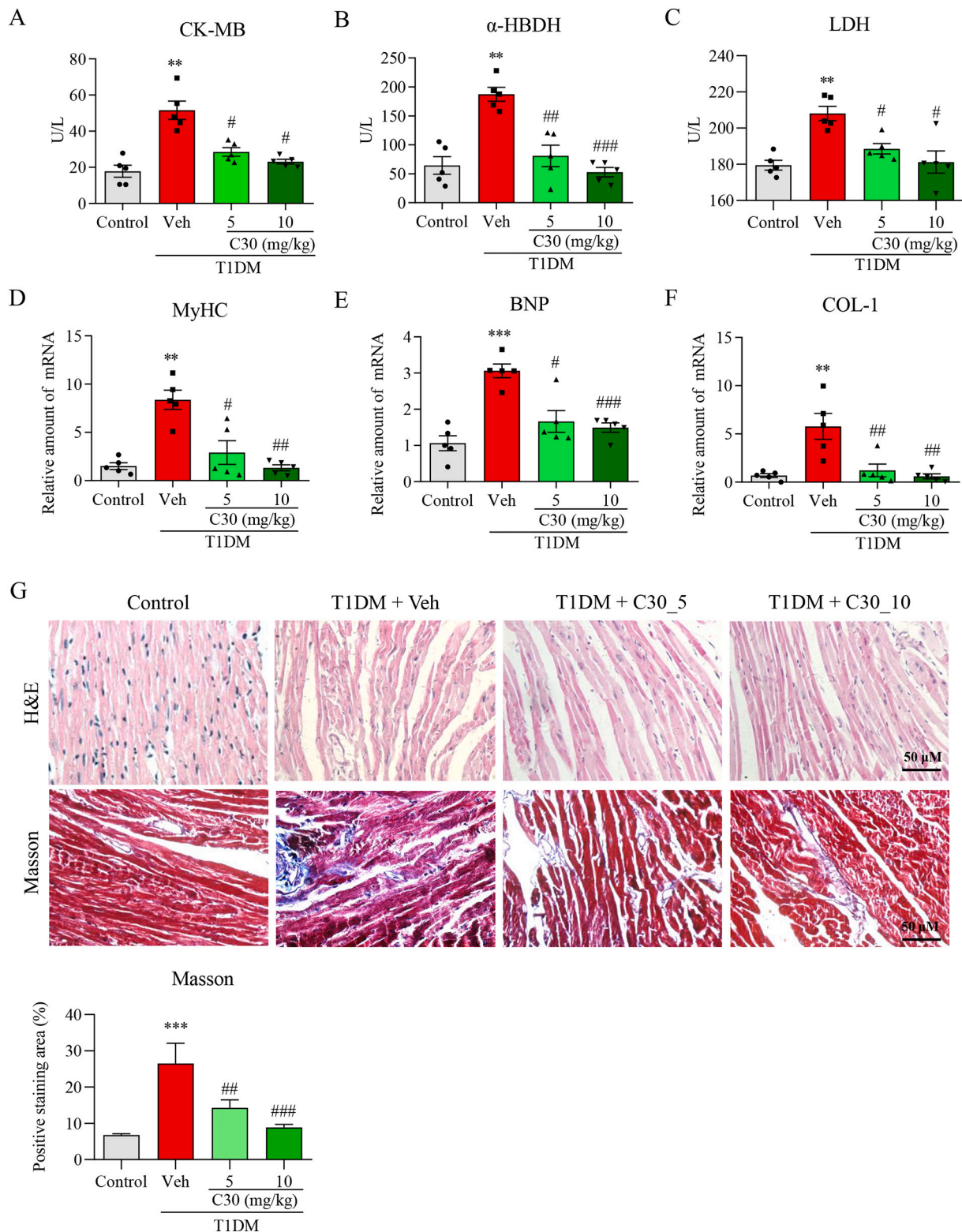


Fig. 5. C30 treatment alleviated myocardial injury in T1DM. T1DM mouse model was induced by STZ injection. The T1DM mice were treated with C30 or vehicle at every other day for 16 weeks by gavage. (A–C) Serum creatine kinase MB (CK-MB), α -hydroxybutyrate dehydrogenase (α -HBDH), and lactate dehydrogenase (LDH) levels were determined. (D–F) MyHC, BNP and COL-1 gene expression in the hearts were determined by real-time quantitative PCR and normalized to the corresponding β -actin level. (G) H&E and Masson's trichrome staining were performed in heart tissue. The representative images (200 \times) were shown and quantified. ** $P < 0.01$, *** $P < 0.001$ vs Control; # $P < 0.05$, ## $P < 0.01$, ### $P < 0.001$ vs vehicle, $n = 5$.

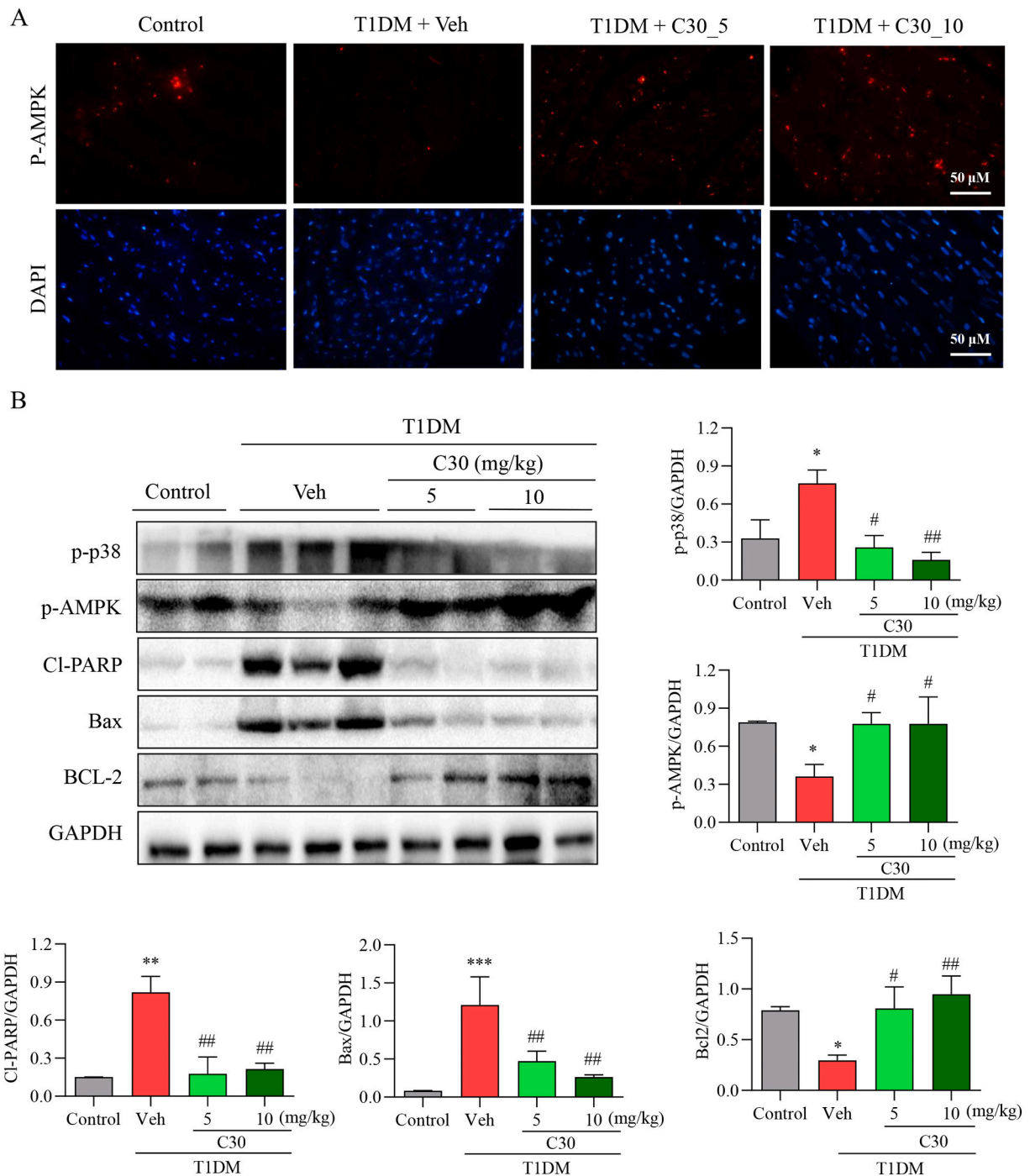


Fig. 6. C30 suppresses hyperglycemia induced cell apoptosis via modulating p38-AMPK axis. (A) Representative images of immunofluorescence staining showed p-AMPK in the heart tissues. (B) p-p38, p-AMPK, cleaved-PARP, Bax, and BCL-2 were detected in the heart tissues by western blot. GAPDH was a loading control. The blots were quantified using Image J. * $P < 0.05$, ** $P < 0.01$, *** $P < 0.001$ vs Control; # $P < 0.05$, ## $P < 0.01$, vs vehicle.

energy metabolic pathway.

Moreover, p38-MAPK activation was identified as an upstream signaling of hyperglycemia-impaired AMPK activation. As a component of MAPKs, p38-MAPK has been shown as a downstream kinase in MD2-TLR4 signaling pathway [44]. Herein, we demonstrated that MD2 inhibition rescued AMPK activity under hyperglycemia condition via p38-MAPK suppression. C30 could not antagonize the inhibitive effect of dorsomorphin on AMPK activation, which further indicated that the effect of C30 on AMPK activation might be through an indirect way.

5. Conclusion

Collectively, MD2 inhibition exhibits therapeutic effects on DCM through p38 MAPK inhibition and AMPK pathway activation in vivo and in vitro, providing a promising target for DCM treatment. In addition, this study demonstrates that C30, as a MD2 inhibitor, significantly inhibits myocardial damage and dysfunction induced by hyperglycemia and identified C30 as a new candidate for the treatment of DCM.

Supplementary data to this article can be found online at <https://doi.org/10.1016/j.bbadis.2022.166369>.

CRedit authorship contribution statement

Jianchang Qian: Conceptualization, Formal analysis, Visualization, Funding acquisition, Writing - Original Draft, Writing - Review & Editing **Fei Zhuang:** Methodology, Investigation, Formal analysis, Data Curation, Visualization **Yujing Chen:** Methodology, Investigation **Xinrong Fan:** Investigation, Data Curation **Jun Wang:** Funding acquisition, Supervision **Zhe Wang:** Resources, Data curation **Yi Wang:** Writing - Original Draft, Writing - Review & Editing **Mingjiang Xu:** Supervision, Writing - Original Draft **Aleksandr V. Samorodov:** Supervision, Writing - Original Draft, Writing - Review & Editing **Valentin N. Pavlov:** Supervision, Writing - Original Draft, Writing - Review & Editing **Guang Liang:** Conceptualization, Supervision, Project administration, Funding acquisition, Writing - Original Draft, Writing - Review & Editing.

Declaration of competing interest

The authors declare that they have no known competing financial interests or personal relationships that could have appeared to influence the work reported in this paper.

Acknowledgments

This study was supported by National Natural Science Foundation of China (81803600 to J.Q., 81970323 to M.X. and 81900331 to Z.W.), Natural Science Foundation of Zhejiang Province (LY18H020013 to J. W.), Zhejiang Provincial Key Scientific Project (2021C03041 to G.L.), the Project of Wenzhou Municipal Science and Technology Bureau (Y20180130 to J.Q. and 2018ZY009 to G.L.), and College Students' Innovation and Entrepreneurship Training Program (202010343018).

References

- [1] W.H. Dillmann, Diabetic cardiomyopathy, *Circ. Res.* 124 (2019) 1160–1162.
- [2] S. Dandamudi, J. Slusser, D.W. Mahoney, M.M. Redfield, R.J. Rodeheffer, H. Chen, The prevalence of diabetic cardiomyopathy: a population-based study in Olmsted County, Minnesota, *J. Card. Fail.* 20 (2014) 304–309.
- [3] S.M. Dunlay, M.M. Givertz, D. Aguilar, L.A. Allen, M. Chan, A.S. Desai, A. Deswal, V.V. Dickson, M.N. Kosiborod, C.L. Lekavich, R.G. McCoy, R.J. Mentz, I.L. Pina, F. American Heart Association Heart, C. Transplantation Committee of the Council on Clinical, Council oncollab <collab>C., N. Stroke, the Heart Failure Society ofcollab <collab>A, Type 2 diabetes mellitus and heart failure: a scientific statement from the American Heart Association and the Heart Failure Society of America: this statement does not represent an update of the 2017 ACC/AHA/HFSA heart failure guideline update, *Circulation* 140 (2019) e294–e324.
- [4] I. Gustafsson, B. Brendorp, M. Seibaek, H. Burchardt, P. Hildebrandt, L. Kober, C. Torp-Pedersen, A. Danish Investigator of, G. Mortality on Dofetilide Study, Influence of diabetes and diabetes-gender interaction on the risk of death in patients hospitalized with congestive heart failure, *Journal of the American College of Cardiology* 43 (2004) 771–777.
- [5] M.R. MacDonald, M.C. Petrie, F. Varyani, J. Ostergren, E.L. Michelson, J.B. Young, S.D. Solomon, C.B. Granger, K. Swedberg, S. Yusuf, M.A. Pfeffer, J.J. McMurray, C. Investigators, Impact of diabetes on outcomes in patients with low and preserved ejection fraction heart failure: an analysis of the candesartan in heart failure: assessment of reduction in mortality and morbidity (CHARM) programme, *Eur. Heart J.* 29 (2008) 1377–1385.
- [6] X. Wang, Y. Wang, V. Antony, H. Sun, G. Liang, Metabolism-associated molecular patterns (MAMPs), *Trends in endocrinology and metabolism: TEM* 31 (2020) 712–724.
- [7] X. Wang, V. Antony, Y. Wang, G. Wu, G. Liang, Pattern recognition receptor-mediated inflammation in diabetic vascular complications, *Med. Res. Rev.* 40 (2020) 2466–2484.
- [8] G. Jia, M.A. Hill, J.R. Sowers, Diabetic cardiomyopathy: an update of mechanisms contributing to this clinical entity, *Circ. Res.* 122 (2018) 624–638.
- [9] Y. Zhang, Y. Li, X. Huang, F. Zhang, L. Tang, S. Xu, Y. Liu, N. Tong, W. Min, Systemic delivery of siRNA specific for silencing TLR4 gene expression reduces diabetic cardiomyopathy in a mouse model of streptozotocin-induced type 1 diabetes, *Diabetes Ther.* 11 (2020) 1161–1173.
- [10] Y. Tan, Z. Zhang, C. Zheng, K.A. Wintergerst, B.B. Keller, L. Cai, Mechanisms of diabetic cardiomyopathy and potential therapeutic strategies: preclinical and clinical evidence, *nature reviewsCardiology* 17 (2020) 585–607.
- [11] Y. Wang, W. Luo, J. Han, Z.A. Khan, Q. Fang, Y. Jin, X. Chen, Y. Zhang, M. Wang, J. Qian, W. Huang, H. Lum, G. Wu, G. Liang, MD2 activation by direct AGE interaction drives inflammatory diabetic cardiomyopathy, *Nat. Commun.* 11 (2020) 2148.
- [12] Y. Wang, Y. Qian, Q. Fang, P. Zhong, W. Li, L. Wang, W. Fu, Y. Zhang, Z. Xu, X. Li, G. Liang, Saturated palmitic acid induces myocardial inflammatory injuries through direct binding to TLR4 accessory protein MD2, *Nat. Commun.* 8 (2017) 13997.
- [13] S. Boudina, E.D. Abel, Diabetic cardiomyopathy, causes and effects, *Rev. Endocrinol. Metab. Disord.* 11 (2010) 31–39.
- [14] H.M. Zhou, Y. Ti, H. Wang, Y.Y. Shang, Y.P. Liu, X.N. Ni, D. Wang, Z.H. Wang, W. Zhang, M. Zhong, Cell death-inducing DFFA-like effector C/CIDEc gene silencing alleviates diabetic cardiomyopathy via upregulating AMPKα phosphorylation, *FASEB J.* 35 (2021), e21504.
- [15] R.A. Elrashidy, S.E. Ibrahim, Cinacalcet as a surrogate therapy for diabetic cardiomyopathy in rats through AMPK-mediated promotion of mitochondrial and autophagic function, *Toxicol. Appl. Pharmacol.* 421 (2021), 115533.
- [16] Q. Yuan, Q.Y. Zhou, D. Liu, L. Yu, L. Zhan, X.J. Li, H.Y. Peng, X.L. Zhang, X. C. Yuan, Advanced glycation end-products impair Na⁽⁺⁾/K⁽⁺⁾-ATPase activity in diabetic cardiomyopathy: role of the adenosine monophosphate-activated protein kinase/sirtuin 1 pathway, *Clin. Exp. Pharmacol. Physiol.* 41 (2014) 127–133.
- [17] Z. Xie, K. Lau, B. Eby, P. Lozano, C. He, B. Pennington, H. Li, S. Rath, Y. Dong, R. Tian, D. Kem, M.H. Zou, Improvement of cardiac functions by chronic metformin treatment is associated with enhanced cardiac autophagy in diabetic OVE26 mice, *Diabetes* 60 (2011) 1770–1778.
- [18] W. Jia, T. Bai, J. Zeng, Z. Niu, D. Fan, X. Xu, M. Luo, P. Wang, Q. Zou, X. Dai, Combined Administration of Metformin and Atorvastatin Attenuates Diabetic Cardiomyopathy by inhibiting inflammation, apoptosis, and oxidative stress in type 2 diabetic mice, *Front. Cell Dev. Biol.* 9 (2021), 634900.
- [19] F. Forcheron, A. Basset, P. Abdallah, P. Del Carmine, N. Gadot, M. Beylot, Diabetic cardiomyopathy: effects of fenofibrate and metformin in an experimental model—the Zucker diabetic rat, *Cardiovasc. Diabetol.* 8 (2009) 16.
- [20] F. Yang, Y. Qin, Y. Wang, S. Meng, H. Xian, H. Che, J. Lv, Y. Li, Y. Yu, Y. Bai, L. Wang, Metformin inhibits the NLRP3 inflammasome via AMPK/mTOR-dependent effects in diabetic cardiomyopathy, *Int. J. Biol. Sci.* 15 (2019) 1010–1019.
- [21] J.H. Kim, J.M. Park, E.K. Kim, J.O. Lee, S.K. Lee, J.H. Jung, G.Y. You, S.H. Park, P. G. Suh, H.S. Kim, Curcumin stimulates glucose uptake through AMPK-p38 MAPK pathways in L6 myotube cells, *J. Cell. Physiol.* 223 (2010) 771–778.
- [22] Z. Cheng, T. Pang, M. Gu, A.H. Gao, C.M. Xie, J.Y. Li, F.J. Nan, J. Li, Berberine-stimulated glucose uptake in L6 myotubes involves both AMPK and p38 MAPK, *Biochim. Biophys. Acta* 1760 (2006) 1682–1689.
- [23] J. Wu, J. Li, Y. Cai, Y. Pan, F. Ye, Y. Zhang, Y. Zhao, S. Yang, X. Li, G. Liang, Evaluation and discovery of novel synthetic chalcone derivatives as anti-inflammatory agents, *J. Med. Chem.* 54 (2011) 8110–8123.
- [24] Y. Wang, X. Shan, G. Chen, L. Jiang, Z. Wang, Q. Fang, X. Liu, J. Wang, Y. Zhang, W. Wu, G. Liang, MD-2 as the target of a novel small molecule, L6H21, in the attenuation of LPS-induced inflammatory response and sepsis, *Br. J. Pharmacol.* 172 (2015) 4391–4405.
- [25] S. Anders, W. Huber, Differential expression analysis for sequence count data, *Genome Biol.* 11 (2010) R106.
- [26] Z. Tian, C. Wang, M. Guo, X. Liu, Z. Teng, An improved method for functional similarity analysis of genes based on gene ontology, *BMC Syst. Biol.* 10 (2016) 119.
- [27] J.H. Joly, W.E. Lowry, N.A. Graham, Differential gene set enrichment analysis: a statistical approach to quantify the relative enrichment of two gene sets, *Bioinformatics* 36 (21) (2020) 5247–5254.
- [28] Y. Wang, Q. Fang, Y. Jin, Z. Liu, C. Zou, W. Yu, W. Li, X. Shan, R. Chen, Z. Khan, G. Liang, Blockade of myeloid differentiation 2 attenuates diabetic nephropathy by reducing activation of the renin-angiotensin system in mouse kidneys, *Br. J. Pharmacol.* 176 (2019) 2642–2657.
- [29] T. Miki, S. Yuda, H. Kouzu, T. Miura, Diabetic cardiomyopathy: pathophysiology and clinical features, *Heart Fail. Rev.* 18 (2013) 149–166.
- [30] G.S. Hotamisligil, Inflammation, metaflammation and immunometabolic disorders, *Nature* 542 (2017) 177–185.
- [31] E. Roh, H.S. Lee, J.A. Kwak, J.T. Hong, S.Y. Nam, S.H. Jung, J.Y. Lee, N.D. Kim, S. B. Han, Y. Kim, MD-2 as the target of nonlipid chalcone in the inhibition of endotoxin LPS-induced TLR4 activity, *J. Infect. Dis.* 203 (2011) 1012–1020.
- [32] H. Gradisar, M.M. Keber, P. Pristovsek, R. Jerala, MD-2 as the target of curcumin in the inhibition of response to LPS, *J. Leukoc. Biol.* 82 (2007) 968–974.
- [33] M.R. Peluso, C.L. Miranda, D.J. Hobbs, R.R. Proteau, J.F. Stevens, Xanthohumol and related prenylated flavonoids inhibit inflammatory cytokine production in LPS-activated THP-1 monocytes: structure-activity relationships and in silico binding to myeloid differentiation protein-2 (MD-2), *Planta Med* 76 (2010) 1536–1543.
- [34] S.Y. Kim, J.E. Koo, Y.J. Seo, N. Tyagi, E. Jeong, J. Choi, K.M. Lim, Z.Y. Park, J. Y. Lee, Suppression of toll-like receptor 4 activation by caffeic acid phenethyl ester is mediated by interference of LPS binding to MD2, *Br. J. Pharmacol.* 168 (2013) 1933–1945.
- [35] B.N. Finck, J.J. Lehman, T.C. Leone, M.J. Welch, M.J. Bennett, A. Kovacs, X. Han, R.W. Gross, R. Kozak, G.D. Lopaschuk, D.P. Kelly, The cardiac phenotype induced by PPARα overexpression mimics that caused by diabetes mellitus, *J. Clin. Invest.* 109 (2002) 121–130.
- [36] Z. Zhang, S. Wang, S. Zhou, X. Yan, Y. Wang, J. Chen, N. Mellen, M. Kong, J. Gu, Y. Tan, Y. Zheng, L. Cai, Sulforaphane prevents the development of cardiomyopathy in type 2 diabetic mice probably by reversing oxidative stress-induced inhibition of LKB1/AMPK pathway, *J. Mol. Cell. Cardiol.* 77 (2014) 42–52.
- [37] Z. Xie, C. He, M.H. Zou, AMP-activated protein kinase modulates cardiac autophagy in diabetic cardiomyopathy, *Autophagy* 7 (2011) 1254–1255.
- [38] M.H. Zou, Z. Xie, Regulation of interplay between autophagy and apoptosis in the diabetic heart: new role of AMPK, *Autophagy* 9 (2013) 624–625.

- [39] A. Woods, P.C. Cheung, F.C. Smith, M.D. Davison, J. Scott, R.K. Beri, D. Carling, Characterization of AMP-activated protein kinase beta and gamma subunits Assembly of the heterotrimeric complex in vitro, *J Biol Chem* 271 (1996) 10282–10290.
- [40] B. Xiao, M.J. Sanders, E. Underwood, R. Heath, F.V. Mayer, D. Carmena, C. Jing, P. A. Walker, J.F. Eccleston, L.F. Haire, P. Saiu, S.A. Howell, R. Aasland, S.R. Martin, D. Carling, S.J. Gamblin, Structure of mammalian AMPK and its regulation by ADP, *Nature* 472 (2011) 230–233.
- [41] R. Abdel Malik, N. Zippel, T. Fromel, J. Heidler, S. Zukunft, B. Walzog, N. Ansari, F. Pampaloni, S. Wingert, M.A. Rieger, I. Wittig, B. Fisslthaler, I. Fleming, AMP-activated protein kinase alpha2 in neutrophils regulates vascular repair via hypoxia-inducible factor-1alpha and a network of proteins affecting metabolism and apoptosis, *Circ. Res.* 120 (2017) 99–109.
- [42] D.T. Eurich, S.R. Majumdar, F.A. McAlister, R.T. Tsuyuki, J.A. Johnson, Improved clinical outcomes associated with metformin in patients with diabetes and heart failure, *Diabetes Care* 28 (2005) 2345–2351.
- [43] S.A. Hawley, R.J. Ford, B.K. Smith, G.J. Gowans, S.J. Mancini, R.D. Pitt, E.A. Day, I.P. Salt, G.R. Steinberg, D.G. Hardie, The Na⁺/Glucose cotransporter inhibitor canagliflozin activates AMPK by inhibiting mitochondrial function and increasing cellular AMP levels, *Diabetes* 65 (2016) 2784–2794.
- [44] G. George, G.L. Shyni, B. Abraham, P. Nisha, K.G. Raghu, Downregulation of TLR4/MyD88/p38MAPK and JAK/STAT pathway in RAW 264.7 cells by *Alpinia galanga* reveals its beneficial effects in inflammation, *J. Ethnopharmacol.* 275 (2021), 114132.